Fusarisetin A, an Acinar Morphogenesis Inhibitor from a Soil Fungus, *Fusarium* sp. FN080326

Jae-Hyuk Jang,[†,▽] Yukihiro Asami,[†,‡,▽] Jun-Pil Jang,[†,▽] Sun-Ok Kim,[†] Dong Oh Moon,[†] Kee-Sun Shin,[‖] Daisuke Hashizume,[⊥] Makoto Muroi,[‡] Tamio Saito,[‡] Hyuncheol Oh,[#] Bo Yeon Kim,*[,§] Hiroyuki Osada,*[,‡] and Jong Seog Ahn*[,†]

[†]Chemical Biology Research Center, Korea Research Institute of Bioscience and Biotechnology (KRIBB), 30 Yeongudanji-ro, Ochang-eup, Cheongwon-gun, Chungbuk 363-883, Republic of Korea

[‡]Chemical Biology Department, RIKEN Advanced Science Institute, 2-1 Hirosawa, Wako-shi, Saitama 351-0198, Japan

[§]World Class Institute, KRIBB, 30 Yeongudanji-ro, Ochang-eup, Cheongwon-gun, Chungbuk 363-883, Republic of Korea

[‖]Biological Resources Center, KRIBB, 125 Gwahak-ro, Yuseong-gu, Daejeon 305-806, Republic of Korea

[⊥]Cooperative Support Team, Advanced Technology Support Division, RIKEN Advanced Science Institute, 2-1 Hirosawa, Wako-shi, Saitama 351-0198, Japan

[#]College of Medical and Life Sciences, Silla University, 100 Silladaehak-gil, Sasang-gu, Busan 617-736, Republic of Korea

S *Supporting Information*

ABSTRACT: An acinar morphogenesis inhibitor named fusarisetin A (**1**) that possesses both an unprecedented carbon skeleton and a new pentacyclic ring system has been identified from an in-house fractionated fungal library using a three-dimensional matrigel-induced acinar morphogenesis assay system. The structure of **1** was determined in detail by NMR and circular dichroism spectroscopy, X-ray analysis, and chemical reaction experiments.

Secondary metabolites produced by microorganisms are a valuable repository of natural bioactive compounds, many of which have been identified as useful research reagents and potential drug candidates. It is often time-consuming and expensive to identify new bioactive molecules using conventional screening strategies. As an alternative approach, we fractionated and screened various fungal extracts using a three-dimensional (3D) epithelial culture system, which allows for the visualization of unique phenotypes such as outgrowth potential, motility, differentiation ability, and morphology formation.[1−3] This screening system uses a gel of reconstituted basement membrane proteins containing growth factors.[4−10] Since the tissue structure and function of epithelial tumors depend on coordinated cues from the extracellular matrix (ECM), neighboring cells, and growth factors[11,12] and because the acquisition of malignancy is generally accompanied by tumor-cell motility, such as acinar morphogenesis, migration, and invasion, this screening approach should aid in the discovery of antitumor reagents related to tumor-cell motility.

In the course of screening our fractionated library, we discovered a fraction derived from the fungus *Fusarium* sp. FN080326 that exhibited inhibitory activity on 3D matrigel-induced acinar morphogenesis of MDA-MB-231 cells. The fungus *Fusarium* sp. FN080326 was isolated from a soil sample collected in Daejeon, Korea. The EtOAc-soluble portion of the fungal extract was purified using flash reversed-phase (ODS) column chromatography followed by reversed-phase HPLC to afford 15 mg of a novel bioactive fungal metabolite named fusarisetin A (**1**; Chart 1).

Compound **1** was obtained as a white powder. The molecular formula $C_{22}H_{31}NO_5$ was determined by analysis of high-resolution electrospray ionization mass spectrometry and NMR data. The IR spectrum displayed absorptions due to hydroxyl groups at 3325 cm^{-1} and carbonyl groups at 1734 and 1666 cm^{-1}. Analysis of ^{13}C, DEPT, and HMQC NMR spectra of **1** confirmed the presence of 22 carbons, including two carbonyl carbons (δ_C 170.9 and 212.9), three quaternary carbons (δ_C 108.5, 75.3, and 55.2), three methyl carbons (δ_C 21.7, 16.6, and 13.2), one *N*-methyl carbon (δ_C 28.8), four methylene carbons (δ_C 60.6, 42.1, 35.3, and 25.4), and nine methine carbons (Table S1 in the Supporting Information). The ^1H NMR spectrum of **1** in CD_3OD indicated the presence of two doublet methyl protons (δ_H 1.47 and 0.94), one singlet methyl proton (δ_H 0.98), one *N*-methyl proton (δ_H 2.97), two mutually coupled olefinic protons (δ_H 5.83 and 5.58, J = 10.0 Hz), two oxymethylene protons (δ_H 3.89 and 3.84), and one oxymethine proton (δ_H 4.37). Additionally, two exchangeable proton signals were observed in DMSO-d_6 at δ 6.69 (s) and 4.57 (s) and assigned as hydroxyl protons (Figure S10 in the Supporting Information). Interpretation of the 2D NMR data, including COSY, HMQC, and HMBC spectra, led to the construction of the planar structure of **1**.

Compound **1** possesses an unprecedented carbon skeleton with a pentacyclic ring system comprising a decalin moiety (6/6) and a tricyclic moiety (5/5/5). The decalin moiety was determined by $^1H-^1H$ COSY and HMBC correlations to be connected from C-7 to C-16, with methyl groups (H$_3$-21 and H$_3$-22) attached at C-12 and C-16, respectively.

The COSY cross-peaks (H$_3$-20/H-5/H-6 and H-3/H-18) and HMBC correlations (H$_3$-20/C-5 and C-6; H-5/C-20; H-6/C-1, C-3, C-5, and C-7; H$_3$-22/C-15, C-16, and C-17; N−CH$_3$/C-2

Chart 1. Structures of Compounds 1−6

1: R₁=R₂=H
2: R₁=H, R₂=Ac
3: R₁=R₂=Ac

4: R₁=R₂=Ac, R₃=R₄=H
5: R₁=R₂=Ac, R₃=p-BrBz, R₄=H
6: R₁=R₂=Ac, R₃=R₄=p-BrBz

Figure 2. X-ray crystal structure of fusarisetin A (**1**).
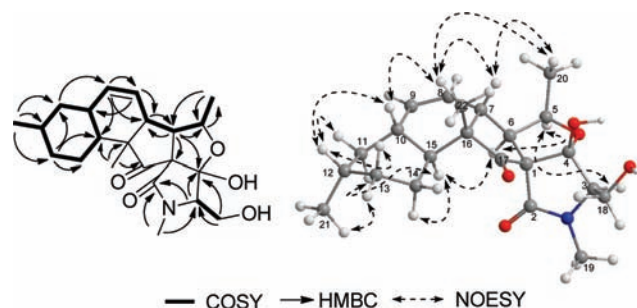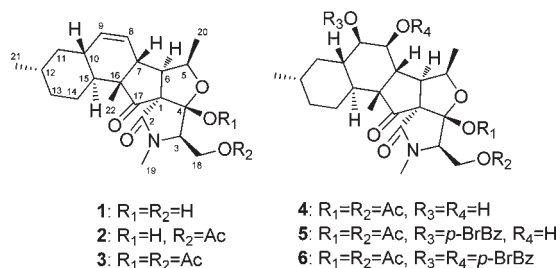

— COSY → HMBC ‹- - -› NOESY

Figure 1. 2D NMR correlations of fusarisetin A (**1**).

and C-3; H-3/C-2 and C-4; H-18/C-3 and C4) were established as a tricyclic moiety, 3a-hydroxy-3-(hydroxymethyl)-2,5-dimethylhexahydro-1H-cyclopenta[3,4]furo[2,3-c]pyrrole-1,8(2H)-dione. Furthermore, the HMBC spectrum in DMSO-d_6 confirmed the location of two hydroxyl groups. C-4 was assigned as a tertiary alcohol on the basis of its carbon chemical shift and an HMBC coupling to an exchangeable proton (δ 6.69 s; 4-OH), which was further coupled to C-3 and C-1. The other hydroxyl group (δ 4.57) was assigned as attached to C-18. Two subunits were connected on the basis of the following 2D NMR correlations: COSY (H-6/H-7/H-8) and HMBC (H₃-22/C-15, C-16 and C-17). Accordingly, the planar structure of **1** was elucidated as shown in Figure 1. The relative stereochemistry of **1** was deduced on the basis of ¹H−¹H coupling constants and NOESY spectroscopic data (Figure 1). The NOESY correlations of H-10 with H-12 and H₃-22 as well as the correlations of H-7 with H₃-20 and H₃-22 indicated that these groups are positioned on the same face, while the correlations of H-15 with H-6 and H-5 with H-6 and H-3 revealed that they are on the opposite face of the molecule. These NOESY data and the relevant coupling constants confirmed the trans junction of the decalin ring system and the cis junction between the tricyclic and decalin ring systems. The configurations of **1** were thereby established except for the configuration at C-1.

Fortunately, **1** was crystallized by slow evaporation from a solution in a 1:1 EtOAc/n-hexane (1:1) mixture over 2 weeks. Although the resulting crystals were not suitable in size and quality for single-crystal X-ray analysis using a laboratory source, data collections performed using a synchrotron source (SPring-8) furnished single-crystal X-ray data that established the relative 3D structure of **1** (Figure 2). The absolute configuration of the chiral centers in **1** was determined by the exciton chirality method[13] using the reduced di-p-bromobenzoate derivative of **1**. After **1** was acetylated, the diacetyl derivative **3** was subjected to OsO₄ oxidation to afford the 8,9-diol derivative (**4**), which was then treated with p-bromobenzoyl chloride in pyridine to furnish the
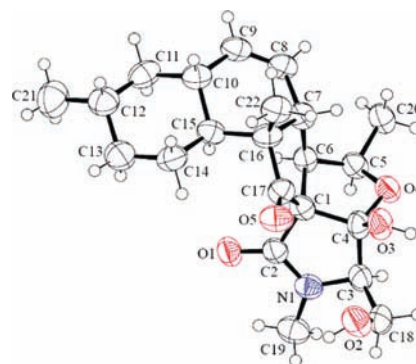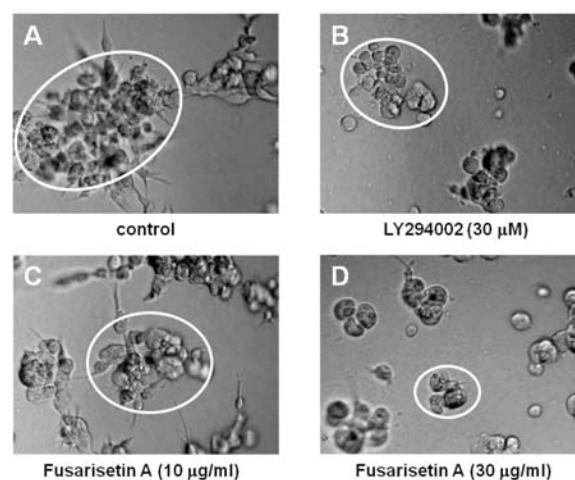

Figure 3. Fusarisetin A (**1**) inhibits 3D matrigel culture-induced colony formation in MDA-MB-231 cells: (A) 3D matrigel control culture; (B) LY294002 (30 μM); (C, D) MDA-MB-231 cells treated with (C) 10 and (D) 30 μg/mL concentrations of **1** for 48 h. Circled areas in the photographs of the control and experimental groups indicate acinar morphogenesis.

8-mono-p-bromobenzoate derivative (**5**) and the 8,9-di-p-bromobenzoate derivative (**6**). The magnitudes of the coupling constants of H-8 (δ 5.85, t, J = 3.2 Hz) and H-9 (δ 5.29, dd, J = 11.2, 3.2 Hz) of **6** confirmed that the p-bromobenzoyl groups at C-8 and C-9 are equatorial and axial, respectively. The circular dichroism (CD) spectrum of **6** exhibited negative first and positive second Cotton effects [$\Delta\varepsilon$ −5.88 (253 nm), +1.86 (238 nm)] (Figure S33). The observed negative exciton chirality indicated the counterclockwise screw sense between the two long axes of the benzoate chromophores, leading to the assignment of the 8S and 9R configurations in **6**. Therefore, the absolute stereochemistries of all the stereogenic centers in **1** were determined as 1S, 3R, 4S, 5R, 6R, 7R, 11R, 12S, 15S, and 16R.

After the structure of fusarisetin A (**1**) was established, the effect of **1** on the cell-based bioassay system was investigated. **1** suppressed the 3D matrigel-induced acinar morphogenesis at a concentration of 30 μg/mL (Figure 3 and Figure S34). In addition, **1** reduced tube formation at the same concentration (Figure S34B,C). To further elucidate the biological effects of **1**, we performed cell migration, cell-growth inhibition, and cell invasion assays using MDA-MB-231 cells. The cell migration was suppressed by **1** at a concentration of 3 μg/mL without any
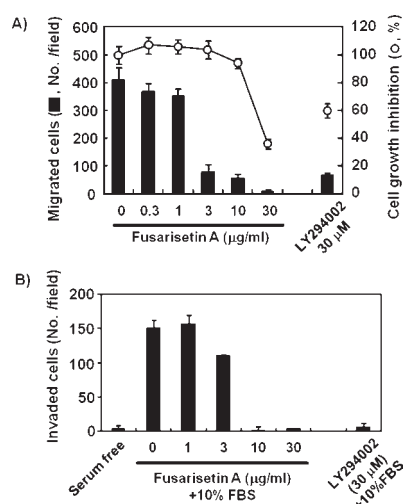
Figure 4. Fusarisetin A (**1**) inhibits cell migration and invasion without cytotoxicity to MDA-MB-231 cells. (A) **1** inhibited cell migration without cytotoxicity at a concentration of 3 μg/mL. Bold bars and open circles show the numbers of migrated cells and extent of cell-growth inhibition, respectively. (B) **1** inhibited serum-induced cell invasion at a concentration of 10 μg/mL. Bold bars show the numbers of invaded cells. LY294002 (30 μM) was used as a positive control.

cytotoxicity, and **1** inhibited serum-induced cell invasion at a concentration of 10 μg/mL (Figure 4 and Figure S35). Additionally, we tested the broad toxic activity of **1** on the same cell line using a cell-growth inhibition assay (data not shown) and flow cytometry analysis (Figure S36). The results showed that **1** did not exhibit any significant inhibition of cell growth or induction of cell death at a concentration of 30 μg/mL. Next, proteomic profiling analysis using the 2D fluorescence difference gel electrophoresis (2D-DIGE) drug targets prediction system was conducted to analyze the key molecule involved in the inhibition of acinar morphogenesis, cell migration, and cell invasion.[14] Interestingly, no similar proteomic profiles were identified when the profile of **1** was compared with those of 19 reference compounds (Figure S37). In addition, no similar patterns of protein variation were observed in comparison with 31 other compounds in our database (data not shown). **1** did not show any inhibitory effect on the phosphorylation of ERK1/2, AKT, p38, or c-Jun in response to epidermal growth factor (EGF) in MDA-MB-231 cells (Figure S38). These results suggested that the molecular target of **1** might be different from those of the reference compounds and is not significantly related to well-known signal pathways for bioactivities. Our findings suggest that **1** inhibits a key process involved in the induction of acinar morphogenesis, cell migration, and invasion in MDA-MB-231 cells.

In conclusion, an acinar morphogenesis inhibitor named fusarisetin A (**1**) that possesses both an unprecedented carbon skeleton and new ring system has been identified from an in-house fractionated fungal library. A literature search identified two previously reported cytochalasin-type fungal metabolites, phomopsichalasin[15] and chaetochalasin A,[16] that might have biosynthetic pathways similar to that of **1** on the basis of their similar pentacyclic ring systems. However, **1** possesses different and unique structural characteristics, such as an *N*-methyl group, a conjugated hexahydrofuro[2,3-*c*]pyrrole unit, a primary alcohol group, and an oxygen-containing isoindol tricyclic moiety (5/5/5) instead of the isoindole tricyclic unit (5/6/5) found in both

phomopsichalasin[15] and chaetochalasin A.[16] Our results show that **1** inhibits a key molecule involved in the development of acinar morphogenesis, cell migration, and invasion in MDA-MB-231 cells. Further studies aimed at the identification of this molecule will provide key insights into the development of antitumor drugs.

■ ASSOCIATED CONTENT

ⓢ Supporting Information. Experimental details, spectral data for compounds, and biological data. This material is available free of charge via the Internet at http://pubs.acs.org.

■ AUTHOR INFORMATION

Corresponding Author
bykim@kribb.re.kr; osadahiro@riken.jp; jsahn@kribb.re.kr

Author Contributions
∇These authors contributed equally.

■ ACKNOWLEDGMENT

■ REFERENCES

(1) Li, J. W.; Vederas, J. C. *Science* **2009**, *325*, 161–165.

(2) Bugni, T. S.; Richards, B.; Bhoite, L.; Cimbora, D.; Harper, M. K.; Ireland, C. M. *J. Nat. Prod.* **2008**, *71*, 1095–1098.

(3) Bugni, T. S.; Harper, M. K.; McCulloch, M. W.; Reppart, J.; Ireland, C. M. *Molecules* **2008**, *13*, 1372–1383.

(4) Krause, S.; Maffini, M. V.; Soto, A. M.; Sonnenschein, C. *BMC Cancer* **2010**, *10*, 263.

(5) Dhimolea, E.; Maffini, M. V.; Soto, A. M.; Sonnenschein, C. *Biomaterials* **2010**, *31*, 3622–3630.

(6) Coppock, H. A.; Gilham, D. E.; Howell, A.; Clarke, R. B. *Cell Proliferation* **2007**, *40*, 721–740.

(7) Shaw, K. R.; Wrobel, C. N.; Brugge, J. S. *J. Mammary Gland Biol. Neoplasia* **2004**, *9*, 297–310.

(8) Debnath, J.; Walker, S. J.; Brugge, J. S. *J. Cell Biol.* **2003**, *163*, 315–326.

(9) Debnath, J.; Muthuswamy, S. K.; Brugge, J. S. *Methods* **2003**, *30*, 256–268.

(10) Muthuswamy, S. K.; Li, D.; Lelievre, S.; Bissell, M. J.; Brugge, J. S. *Nat. Cell Biol.* **2001**, *3*, 785–792.

(11) Wang, F.; Hansen, R. K.; Radisky, D.; Yoneda, T.; Barcellos-Hoff, M. H.; Petersen, O. W.; Turley, E. A.; Bissell, M. J. *J. Natl. Cancer Inst.* **2002**, *94*, 1494–1503.

(12) Debnath, J.; Brugge, J. S. *Nat. Rev. Cancer* **2005**, *5*, 675–688.

(13) Harada, N.; Nakanishi, K. *Acc. Chem. Res.* **1972**, *5*, 257–263.

(14) Muroi, M.; Kazami, S.; Noda, K.; Kondo, H.; Takayama, H.; Kawatani, M.; Usui, T.; Osada, H. *Chem Biol.* **2010**, *17*, 460–470.

(15) Horn, W. S.; Simmonds, M. S. J.; Schwartz, R. E.; Blaney, W. M. *Tetrahedron* **1995**, *51*, 3969–3978.

(16) Oh, H.; Swenson, D. C.; Gloer, J. B. *Tetrahedron Lett.* **1998**, *39*, 7633–7636.